

Tetrakis(4-phenylbutyl) ester 2g, mp 152.5–155 °C, (EtOAc), the minor component, had δ 7.463 (1 H, s, Ar'H), 7.18–7.31 (5 H, m, ArH), 4.876 (1 H, d, $J = 17$ Hz, $\text{CH}_A\text{C}\equiv\text{C}$), 4.662 (1 H, d, $J = 17$ Hz, $\text{CH}_B\text{C}\equiv\text{C}$), 4.3 (2 H, m, COOCH_2), 2.66 (2 H, m, CH_2Ar), 1.76 (4 H, m, CH_2). The more soluble isomer of **2g** displayed an AB quartet ($\text{CH}_{A,B}\text{C}\equiv\text{C}$) centered at δ 4.79 ($J_{AB} = 17$ Hz, $\Delta\nu_{AB} = 38$ Hz).

The less soluble isomer of tetrakis(5-phenylpentyl) ester **2h**, mp 138.5–9.5 °C (acetone), equilibrated very rapidly to a mixture of syn and anti isomers at 25 °C with distinctive aromatic singlet absorptions at δ 7.441 and 7.449 and two AB quartets ($\text{CH}_{A,B}\text{C}\equiv\text{C}$, $J_{AB} = 17$ Hz) centered at δ 4.708 ($\Delta\nu_{AB} = 58$ Hz), and δ 4.730 ($\Delta\nu_{AB} = 36$ Hz). When dissolved at a temperature lower than –14 °C, the spectrum appeared to be primarily that of a single compound corresponding to the minor component of the mixture, with δ 7.446 (1 H, s, Ar'H), 7.19–7.933 (5 H, m, ArH), 4.821 (1 H, d, $J = 17$ Hz, $\text{CH}_A\text{C}\equiv\text{C}$), 4.607 (1 H, d, $J = 16.9$ Hz, $\text{CH}_B\text{C}\equiv\text{C}$), 4.29 (2 H, m, COOCH_2), 2.64 (2 H, t, $J = 7.7$ Hz, CH_2Ar), 1.46–1.74 (6 H, m, CH_2).

Both isomers of tetracinnamyl ester **2i**, could be isolated by fractional crystallization. The less soluble isomer, mp 166.5–170 °C (EtOAc-hexane), had δ 7.498 (1 H, s, Ar'H), 7.2–7.5 (5 H, m, ArH), 6.756 (1 H, d, $J = 16$ Hz, $\text{CH}=\text{CHAr}$), 6.400 (1 H, dt, $J = 16, 6.3$ Hz, $\text{CH}_2\text{CH}=\text{CH}$), 4.991 (1 H, ddt, $J = 13, 6.3, 1.2$ Hz, $\text{COOCH}_A\text{CH}=\text{CH}$), 4.931 (1 H, ddt, $J = 13.6, 6.3, 1.2$ Hz, $\text{COOCH}_B\text{CH}=\text{CH}$), 4.876 (1 H, d, $J = 17$ Hz, $\text{CH}_A\text{C}\equiv\text{C}$), 4.650 (1 H, d, $J = 17$ Hz, $\text{CH}_B\text{C}\equiv\text{C}$). The more soluble isomer of **2i**, decomposition without melting above 200 °C, had δ 7.527 (1 H, s, Ar'H), 7.2–7.5 (5 H, m, ArH), 6.738 (1 H, d, $J = 16$ Hz, $\text{CH}=\text{CHAr}$), 6.371 (1 H, dt, $J = 16, 6.3$ Hz, $\text{CH}_2\text{CH}=\text{CH}$), 4.991 (1 H, ddt, $J = 12.5, 6.3, 1.2$ Hz, $\text{CH}_A\text{CH}=\text{CH}$), 4.888 (1 H, ddt, $J = 12.5, 6.3, 1.2$ Hz, $\text{CH}_B\text{CH}=\text{CH}$), 4.913 (1 H, d, $J = 17$ Hz, $\text{CH}_A\text{C}\equiv\text{C}$), 4.689 (1 H, d, $J = 17$ Hz, $\text{CH}_B\text{C}\equiv\text{C}$).

Hexadecahydro Derivatives 3. Tetraacid **3j** was obtained by hydrolysis of the tetraethyl ester (**3**, R = Et),⁸ using excess lithium hydroxide in 50% aqueous THF. A suspension of 104 mg (0.19 mM) of **3j**, 197 mg (0.75

mM) of triphenylphosphine, and 111 mg (1.0 mM) of benzyl alcohol in THF was treated with 129 mg (0.74 mM) of diethyl azodicarboxylate. Crystallization of the crude product obtained after chromatography afforded 59 mg of tetrabenzyl ester **3a**, mp 159.5–162 °C (EtOAc-hexane), in 54% yield: H NMR δ 7.3–7.5 (5 H, m, Ar'H), 6.852 (1 H, s, Ar'H), 5.407 (1 H, d, $J = 12$ Hz, CH_AAr), 5.139 (1 H, d, $J = 12$ Hz, CH_BAr), 3.4–3.5 (2 H, m, OCH_2CH_2), 1.7 and 1.3 (2 H, m, $\text{OCH}_2\text{CH}_2\text{CH}_2$), 1.0 (2 H, m, $\text{OCH}_2\text{CH}_2\text{CH}_2$).

Tetraphenylpropyl ester 3f, was obtained in low yield as a colorless oil by a similar procedure: H NMR δ 7.1–7.3 (5 H, m, Ar'H), 7.038 (1 H, s, Ar'H), 4.291 (1 H, dt, $J = 11, 7$ Hz, COOCH_A), 4.242 (1 H, dt, $J = 11, 7$ Hz, COOCH_B), 4.1 and 3.9 (2 H, m, Ar'OCH₂), 2.731 (2 H, t, $J = 8$ Hz, CH_2Ar), 2.0–2.1 (2 H, m, $\text{CH}_2\text{CH}_2\text{CH}_2\text{Ar}$), 1.4–2.0 (4 H, unassigned).

Interconversion of Syn–Anti Isomers. Except for 2-phenethyl ester **2e**, the less soluble isomer isolated from the cupric acetate cyclizations was the less stable isomer as determined by direct equilibration. The rate of equilibration was determined by observing changes in its proton spectra. For those interconversions that were inconveniently rapid at room temperature (**2e–h**), rates were determined at lower temperatures in a Bruker WH-270 spectrometer equipped with a liquid nitrogen cooled variable temperature probe. The probe temperature was determined (calibrated thermocouple) before and after a series of spectra. The temperature deviation during the time of a kinetic run was generally less than 0.5 °C. Rates of those interconversions that were slow at room temperature (**2a–d, i**) were determined by immersing a sealed NMR tube in a constant temperature bath and removing the sample periodically for proton spectra at 22 °C. Peak areas were determined by digital integration with the aid of an overlapping Lorentzian deconvolution program as appropriate. Peak areas were insensitive to variations in the spectrometer's pulse delay. Rate constants and the corresponding half-lives were extracted by treating the interconversions as reversible first-order processes (Table I).

Photochemistry of 1-Azatriptycene

Tadashi Sugawara and Hiizu Iwamura*

Contribution from the Department of Applied Molecular Science, Institute for Molecular Science, Myodaiji, Okazaki 444, Japan. Received October 20, 1983.

Revised Manuscript Received June 4, 1984

Abstract: 1-Azatriptycene (**1**) underwent photorearrangement in basic methanol with a quantum efficiency of 0.57 to give 4*H*-azepine derivative (**4**) as the main product. In the presence of TCNE, the Diels–Alder adduct (**5**) of the 1*H*-azepine intermediate was obtained. In acetic acid, a further photoreaction of the initially formed indenoacridine (**9**) gave the dihydromethyl derivative (**10**). The structures were established by spectral data. The 4*H*-azepine **4** was converted to the azepinium salt (**6**) by hydride abstraction. The observed photochemistry is interpreted in terms of the formation of 2-(9-fluorenyl)phenylnitrene (**3**). When 2-(9-fluorenyl)phenyl azide (**2**) was photolyzed with the purpose of generating **3** independently, the yields of **4**, **5**, and **9** were lower and some additional products were obtained. The difference in reactivity was more evident in the reactions of **1** and **2** in low-temperature matrices as monitored by UV absorptions and is interpreted in terms of the different conformation of **3**: the ap conformation of the initially formed **3a** from **1** and the sp form from **2**. The crossover of the photoproducts is presumably due to conformational interconversion from **3b** to **3a** through intermediate **17** formed by insertion of the phenylnitrenic center into its own ring. Irradiation of **1** and **2** at 4.2 K in methylcyclohexane glass in an ESR cavity showed a strong signal due to the X, Y transition of triplet **3**. The resonance field was again slightly different, corroborating the different conformations **3a** and **3b** from **1** and **2**, respectively. The ESR spectrum obtained by irradiation of **1** did not contain any signal due to a phenylcarbene but a set of signals due to a triplet species with the smaller D parameter. The latter was assigned to diradical **18** formed by the C–N bond cleavage as a side reaction. Diversion from a typical di- π -methane rearrangement route and the bridging regioselectivity are discussed. Lastly, the fluorescence and $S_n \leftarrow S_1$ absorption spectra of triptycenes were scrutinized to show that the fluorescent state is different from the Franck–Condon state and more like the excimer of xylenes.

Intramolecular interaction between benzene moieties plays an important role in the photophysics of aromatic polychromophoric systems in the photoexcited state.¹ One very well explored case is [2.2]paracyclophane, in which two benzene rings have a parallel orientation with a maximum overlap of the p orbitals and where an intramolecular charge-transfer band is observed in its absorption

spectrum.^{1c} The photolysis of the cyclophane in alcohols gives photosolvolytic products through the singlet state with a charge-transfer character, together with 1,2-diphenylethane derivatives through the triplet excited state.^{2a} The reactivity can

(1) (a) Klöpffer, W. "Organic Molecular Photophysics"; Birks, J. B., Ed.; Wiley: New York, 1973; Vol. 1, p 357. (b) Kaupp, G. *Angew. Chem., Int. Ed. Engl.* **1980**, *19*, 243. (c) Iwata, S.; Fuke, K.; Sasaki, M.; Nagakura, S.; Otsubo, T.; Misumi, S. *J. Mol. Spectrosc.* **1973**, *46*, 1. (d) Nakashima, N.; Sumitani, M.; Ohmine, I.; Yoshihara, K. *J. Chem. Phys.* **1980**, *72*, 2226.

(2) (a) Helgeson, R. C.; Cram, D. J. *J. Am. Chem. Soc.* **1966**, *88*, 509. (b) Ishikawa, S.; Nakamura, J.; Iwata, S.; Sumitani, M.; Nagakura, S.; Sakata, Y.; Misumi, S. *Bull. Chem. Soc. Jpn.* **1979**, *52*, 1346. (c) Ishikawa, S.; Nakamura, J.; Nagakura, S. *Ibid.* **1980**, *53*, 2476. (d) Ishikawa, S.; Nakamura, J.; Nagakura, S. *Ibid.* **1981**, *54*, 685. (e) Schweitzer, D.; Colpa, J. P.; Behnke, J.; Hauser, K. H.; Haenel, M.; Staab, H. A. *Chem. Phys.* **1975**, *11*, 373. (f) Colpa, J. P.; Hauser, K. H.; Schweitzer, D. *Ibid.* **1978**, *29*, 187.

Table I. Conditions and Products of Irradiations of **1** and **2**

run no.	substrate (concn mM)	solvent	temp, °C	additive	conversion, %	product distribution, %							
						4	5	13	9	10	16	14	15
1	1 (1.40)	CH ₃ OH	25	CH ₃ ONa ^a	66	69			0		0		
2	2 (0.40)	CH ₃ OH	25	CH ₃ ONa ^a	72	34			0		0		
3	1 (1.34)	CH ₃ CN	25	TCNE ^b	73	0	74	0	5		0		
4	1 (1.35)	CH ₃ CN	-40	TCNE ^b	37	0	45	0	2		0		
5	2 (1.31)	CH ₃ CN	25	TCNE ^c	62	0	42	16	0.5		0		
6	2 (1.30)	CH ₃ CN	-40	TCNE ^c	42	0	14	69	0		0		
7	1 (1.05)	CH ₃ CN	25	Et ₂ NH ^d	77	47			0		0	0	0
8	2 (2.70)	Et ₂ NH	25		>95	0			0			10	25
9	1 (0.51)	AcOH	25		24	0			60		7	6	
10	1 (0.51)	AcOH	25		>95	0			8		48	10	
11	1 ·HCl (0.51)	CH ₃ CN	25		64	0			49		0		

^a 4.35 mM. ^b 2.67 mM. ^c 2.70 mM. ^d 0.40 mM.

Table II. ¹H Chemical Shifts and Coupling Data for the TCNE Adducts of 1*H*-Azepine Derivatives

	δ				J , Hz			
	H ₃	H ₄ ^a	H ₅	H ₆	J_{45}	J_{34}	J_{56}	J_{35}
5	6.76	5.04	3.92	7.02	8.5	8.2	6.6	3.0
Aa ⁷	7.1	5.22	3.92	6.55	8.8	8.8	8.1	
Ab ⁷	6.63		3.16	6.33			7.7	1.1
Ac ⁷	6.93	5.22	3.80		9.0	9.2		

^a The β -H of the enamines characteristically at high field.

be rationalized by the interaction between the benzenoid chromophores and by the favorable σ - π overlap between the strained bridging C-C bonds and p orbitals of the benzene rings. A spectroscopic detection has also been reported on ethylenebis-(benzyl) diradical formed from a higher triplet state.^{2b-d} Triptycene, which has three benzene rings in threefold symmetry, provides another intriguing molecular framework. Although the three benzene rings are fixed at 120° angles to each other and apparently located in a less favorable orientation for overlapping of the p orbitals, interaction of reasonable strength is evident in UV and CD spectra.³ As a chemical consequence of the excitonic interaction of the degenerate chromophoric system in triptycenes, they undergo direct bonding between two of the three benzene rings to extrude a bridgehead atom as a monocentric diradical species.⁴ This reactivity is considered to be parallel with the incipient di- π -methane rearrangement through which photoisomerization of mono- and dibenzobarrelene takes place,⁵ but it shows a contrasting diversion therefrom in the subsequent stages. In order to examine the generality and the selectivity of this photorearrangement, photolysis of 1-azatriptycene (**1**), where one of the bridgehead carbon atoms of triptycene is replaced by nitrogen, has been investigated extensively.⁶

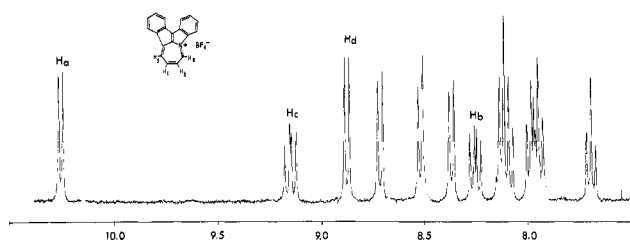
This paper deals with the mechanistic details of the photorearrangement of **1** based on analyses of photoproducts, detection of the nitrene intermediacy by low-temperature ESR spectroscopy,

(3) (a) Wilcox, C. F., Jr. *J. Chem. Phys.* **1960**, *33*, 1874. (b) Wilcox, C. F., Jr.; Craig, A. C. *J. Org. Chem.* **1961**, *26*, 249. (c) Harada, N.; Tamai, Y.; Takuma, J.; Uda, H. *J. Am. Chem. Soc.* **1980**, *102*, 501. (d) Harada, N.; Tamai, Y.; Uda, H. *Ibid.* **1980**, *102*, 506.

(4) (a) Walsh, T. D. *J. Am. Chem. Soc.* **1969**, *91*, 515. (b) Turro, N. J.; Tobin, M.; Friedman, L.; Hamilton, J. B. *Ibid.* **1969**, *91*, 516. (c) Iwamura, H.; Yoshimura, K. *Ibid.* **1974**, *96*, 2652. (d) Iwamura, H.; Tukada, H. *Tetrahedron Lett.* **1978**, 3451. (e) Kawada, Y.; Tukada, H.; Iwamura, H. *Ibid.* **1980**, *21*, 181. (f) Tukada, H.; Iwamura, M.; Sugawara, T.; Iwamura, H. *Org. Magn. Reson.* **1982**, *19*, 78.

(5) For reviews see: (a) Hixon, S. S.; Mariano, P. S.; Zimmerman, H. E. *Chem. Rev.* **1973**, *73*, 531. (b) Zimmerman, H. E. "Rearrangements in Ground and Excited States"; de Mayo, P., Ed.; Academic Press: New York, 1981; Vol. 3, p 131. (c) Zimmerman, H. E.; Grunewald, G. L. *J. Am. Chem. Soc.* **1966**, *88*, 183. (d) Zimmerman, H. E.; Binkley, R. W.; Givens, R. S.; Sherwin, M. A. *J. Am. Chem. Soc.* **1967**, *89*, 3932. (e) Zimmerman, H. E.; Givens, R. S.; Pagni, R. M. *Ibid.* **1968**, *90*, 6909. (f) Ciganek, E. *Ibid.* **1966**, *88*, 2882. (g) Richards, K. E.; Tillman, R. W.; Wright, G. J. *Aust. J. Chem.* **1975**, *28*, 1289. (h) Paddick, R. G.; Richards, K. E.; Wright, G. J. *Ibid.* **1976**, *29*, 1005. (i) Iwamura, M.; Tukada, H.; Iwamura, H. *Tetrahedron Lett.* **1980**, *21*, 4865. For discussion of electronegativity at the methane position see: (j) Zimmerman, H. E.; Armesto, D.; Amezu, M. C.; Gannett, T. P.; Johnson, R. P. *J. Am. Chem. Soc.* **1979**, *101*, 6367.

(6) (a) Sugawara, T.; Iwamura, H. *J. Am. Chem. Soc.* **1980**, *102*, 7134. (b) Sugawara, T.; Nakashima, N.; Yoshihara, K.; Iwamura, H. *Ibid.* **1983**, *105*, 859.

**Figure 1.** The 360-MHz NMR spectrum of azepinium tetrafluoroborate (**6**) in CD₃CN.**Table III.** ¹H NMR Data for Azepinium Salt **6** and the Related Compounds

	DBH	6	7	8
H _a ^b	8.50	10.26	7.85	8.63
H _b ^b	7.94	8.25	6.18	6.87
H _c ^b	7.94	9.15		
H _d ^b	8.50	8.89	7.20	(7.8) ^a
J_{ab}^c	5.7	7.9	10.0	9.6
J_{bc}^c		11.8		
J_{cd}^c	5.7	8.8		
J_{ac}^c	3.3	>1.0		
J_{bd}^c	3.3	2.0	1.9	2.2

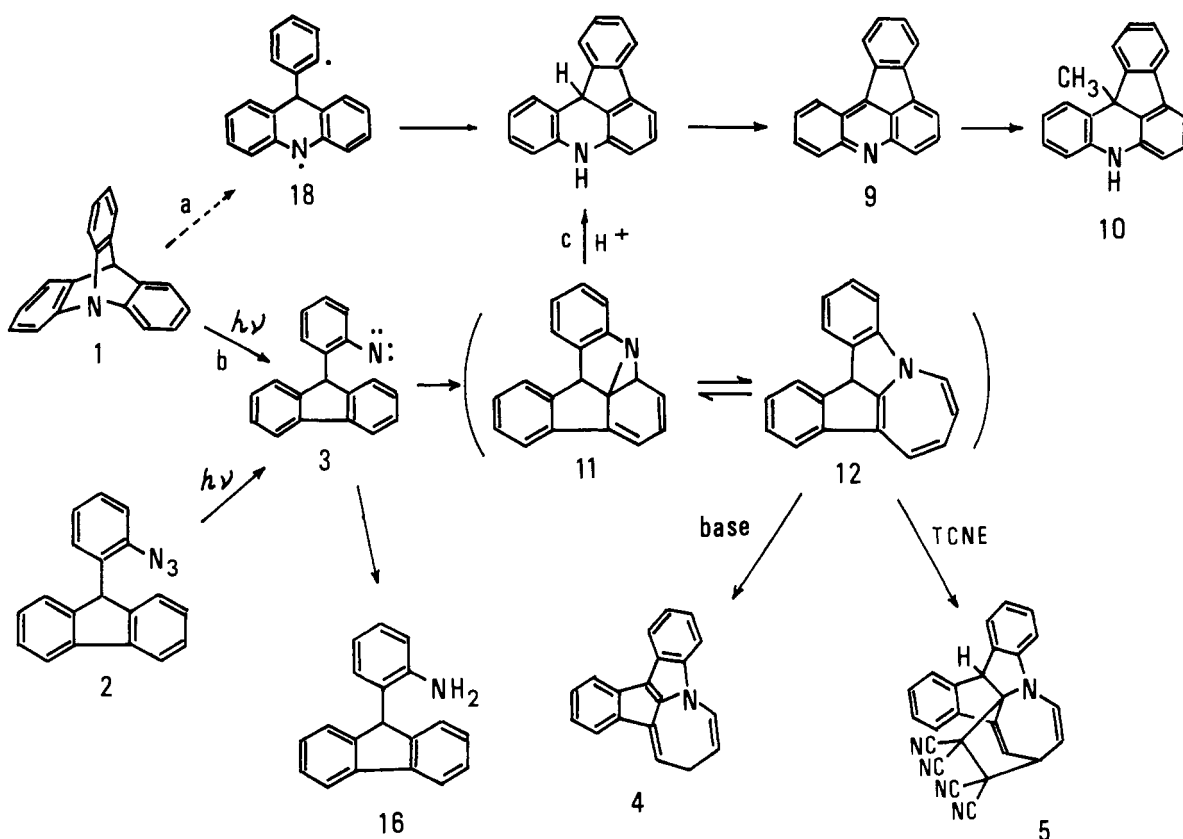
^a Overlapped with one of the aromatic protons. ^b ppm. ^c Hz.

and characterization by means of emission and absorption spectroscopy of its singlet excited state from which monocentric diradical species are generated in high efficiency.

Results and Discussion

(a) **Photoproducts of 1-Azatriptycene (1).** The photoreactions of **1** were carried out with a low-pressure mercury lamp under various conditions, and a number of new products due to nitrene **3** were characterized. The results are summarized in Table I (see Scheme I). After irradiation of a dilute methanolic solution in the presence of a small amount of methoxide (4.35 mM), azepine derivative (**4**) was isolated as orange needles in 69% yield. The 100-MHz ¹H NMR of **4** showed three olefinic protons, A, B, and C at δ 4.7 (m, 10- and 4.5-Hz coupling with C and D signals,

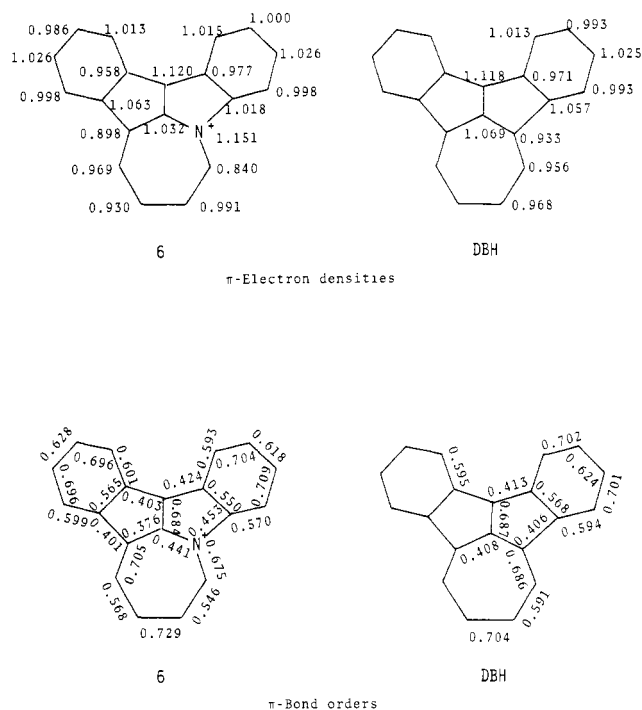
Scheme 1



respectively), 6.3 (t, 4.2-Hz coupling with D), and 6.7 (d, 10-Hz coupling with A), respectively, and two methylene protons D at δ 3.8 (triplet-like, 4.5- and 4.2-Hz couplings with signals A and B, respectively) in addition to the aromatic multiplets at δ 7.0–7.8. The coupling pattern is consistent with the partial structure $N-CH^C=CH^A-CH_2^D-CH^B=$. The formation of 3*H*-azepine derivative 4 can be rationalized by a base-promoted isomerization of 1*H*-azepine (12), which is in equilibrium with azanocaradiene (11). The latter should be formed by the intramolecular addition of *o*-fluorenylphenylnitrene (3) which may be derived from 1 through a photoextrusion reaction of the bridgehead nitrogen atom (vide infra).

Hydride abstraction from 4 by trityl tetrafluoroborate in chloroform gave a stable azepinium salt (6), as dark brown needles, which was well characterized by 360-MHz 1H NMR (Figure 1). A characteristic downfield shift of the α proton (H_a) of the azepine ring (δ 10.26) suggests the iminium ion character of 6.⁷ Since azepinium salt 6 is isoelectronic with the dibenzo (Hafner's hydrocarbon) recently reported,^{3c} their chemical shifts are compared in Table III. The π -electron density and bond order of dibenzo (Hafner's compound) and 6 have also been calculated by means of the PPP MO method in order to confirm the 1H NMR spectral assignments (Figure 2). The calculated π -electron densities of the hydrocarbon compound indicated a fulvene-type charge distribution; a positive charge is accumulated in the seven-membered ring, leaving a negative charge in the five-membered rings. The positive charge on the nitrogen atom in 6 is partially neutralized by π conjugation in the seven-membered ring. The π -electron density on each carbon atom of the azepinium ring correlates the observed 1H NMR chemical shifts by ca. 10 ppm/ π electron.

In addition to azepine derivative 4, an oxidized product, azepinone derivative 7, was obtained as a byproduct in low yield. The IR absorption band at 1635 and 1600 cm^{-1} and the ^{13}C NMR signal at δ 187.8 indicate the presence of an amide linkage. The 1H NMR spectrum shows an AB quartet at δ 6.18 and 7.85 with



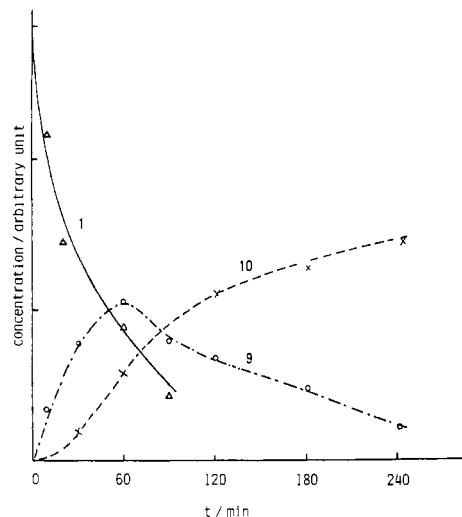
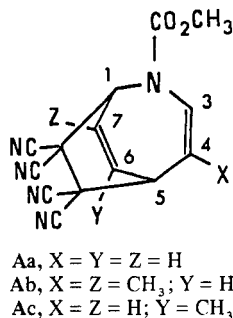


Figure 3. Appearance of the products and disappearance of the starting material during the irradiation of 1-azatriptcene (**1**) in acetic acid ($c = 0.51$ mM).

structure. The wine red color of **7** in chloroform ($\delta_{\max}(\epsilon)$ 379 (4.71), 325 (4.17), 352 [sh] (3.99), 504 (2.74)) changed to green in trifluoroacetic acid ($\lambda_{\max}(\epsilon)$ 308 (3.75), 319 (3.76), 346 (3.73), 360 [sh] (3.71), 425 (3.36), 448 [sh] (3.29), 655 (2.29)). The change in color is presumably due to protonation at the carbonyl oxygen to give the hydroxyazepinium ion **8**. The process was also monitored by ^1H NMR spectroscopy (see Table III). The smaller downfield shift of the H_a proton of the azepinium ring of **8** compared with that of **6** indicates that the distribution of the positive charge was now between the lone pairs of electrons on the nitrogen and oxygen atoms.

The photolysis was carried out in acetonitrile in the presence of TCNE to give an adduct **5**, colorless plates [a parent peak at m/e 383 and a base peak at m/e 255 ($\text{M}^+ - 128$ (TCNE))] (runs 3 and 4 in Table I). The marked similarity of the ^1H NMR spectrum of **5** to those of other TCNE adducts of 1*H*-azepine derivatives (Aa–Ac) in the literature⁸ leaves no doubt that the assigned structure is correct (Table II). The formation of **5** indicates that 1*H*-azepine **12** was trapped externally with TCNE.

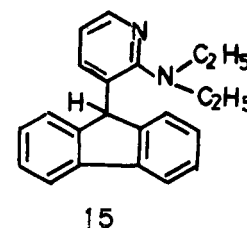
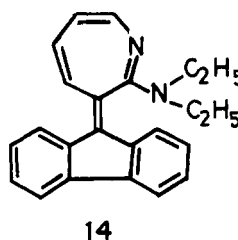
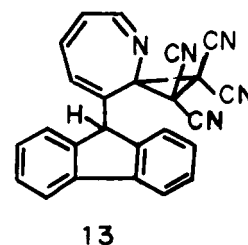


Since fluorescence was effectively quenched by the addition of diethylamine (vide infra), the photorearrangement of **1** was studied in the presence of a low concentration (4×10^{-4} M) of the amine; **4** was obtained as the sole product (run 7 in Table I).

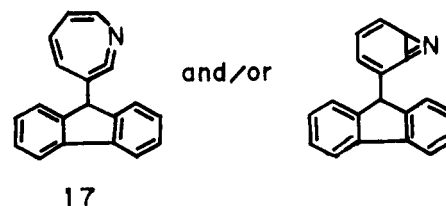
When **1** was irradiated in acetic acid, indenoacridine (**9**) was obtained as described in the literature.⁹ However, **9** was photolabile under these conditions and gave the 12*b*-methyl-5,12*b*-dihydro derivative **10** as a secondary product (runs 9 and 10 in Table I). Formation of **9** in acetic acid was interpreted as arising from the C–N bond cleavage followed by free radical phenylation (route a in Scheme I) by Wittig and Steinhoff, who prepared **1** for the first time in 1964 via internal nucleophilic cycloaddition

of a benzyne.⁹ Thus, the irradiation of **1** in acetic acid was monitored by HPLC to give the results in Figure 3. The concentration of **9** reached a maximum at 65 min and then started to decrease, while that of **10** increased thereafter. According to the known photochemical behavior of acridine, **10** can be reasoned as being formed from the ion pair consisting of the conjugate acid of **9** and acetate anion produced from the photoexcited state of **9**. Electron transfer followed by decarboxylation and recombination would give **10**.¹⁰ Combining the above findings, the formation of **9** and **10** should better be interpreted in terms of the intermediacy of nitrene **3** (route b in Scheme I) rather than diradical **18** formed through a one C–N bond cleavage. Azanorcaradiene (**11**), which is in equilibrium with 1*H*-azepine (**12**),¹¹ isomerizes to dihydroacridine through C–N bond fission under acidic conditions, and the latter is autoxidized to give **9**.

(b) Photolysis of Azide 2. In order to verify the above reaction sequences, nitrene **3** was generated independently by the photolysis of azide **2** to give similar results but with slightly different distributions (see Table I). In run 2, for example, the yield of **4** is about one-half of that of the photorearrangement of **1**. The difference is enhanced when the photoreactions at lower temperatures are compared (runs 4 and 6). These discrepancies could be attributed to different spin state and/or conformations of nitrene **3** generated from **1** and **2** (vide infra). Besides azepine–TCNE



adduct **5**, another TCNE adduct (**13**) was obtained. This adduct was not stable and resisted further purification. An imine proton was observed at δ 8.34 in ^1H NMR with a small coupling constant ($J = 2$ Hz), and the fluorenyl ring appeared to be intact in **13**. Decoupling experiments revealed the presence of four consecutive olefinic protons on the azepine ring, two of which overlapped at δ 7.0. The parent peak in the mass spectrum (M^+ 383, 45.1%) corresponded to the fluorenylazepine–TCNE 1:1 adduct. The fragmentation pattern was, however, different from normal TCNE–azepine adducts and gave a peak at m/e 318 corresponding to $\text{M}^+ - \text{CH}(\text{CN})_2$ (57.5%). The product should be formed through an external trapping of an azirine and/or azacycloheptatetraene (**17**) by TCNE. Namely, insertion into its own phenyl



(8) (a) Baldwin, J. E.; Smith, R. A. *J. Am. Chem. Soc.* **1965**, *87*, 4819. (b) Paquette, L. A.; Kuhla, D. E.; Barrett, J. H.; Leichter, L. M. *J. Org. Chem.* **1969**, *34*, 2888.

(9) Wittig, G.; Steinhoff, G. *Liebigs Ann. Chem.* **1964**, *676*, 21.

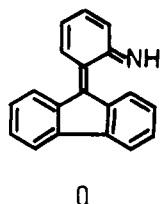
(10) (a) Kira, A.; Kato, S.; Koizumi, M. *Bull. Chem. Soc. Jpn.* **1966**, *39*, 1221. (b) Castellano, A.; Catteau, J. P.; Lablache-Combiere, A.; Allan, G. *Can. J. Chem.* **1973**, *51*, 3508. (c) Vermeersch, G.; Febray-Garot, N.; Caplain, S.; Lablache-Combiere, A. *Tetrahedron* **1975**, *31*, 867.

(11) Vogel, E.; Altenbach, H.-J.; Drossard, J.-M.; Schmickler, H.; Stegelmeier, H. *Angew. Chem., Int. Ed. Engl.* **1980**, *19*, 1016.

ring must have taken place in *o*-fluorenylphenylnitrene to give valence isomer **17**. Either one of [2 + 2] and [2 + 4] cycloadducts between **17** and TCNE does not account for the coupling pattern. Spectral data suggest the structure carrying a spiro-tetracyano-cyclopropane ring at the 2 position on the 2*H*-azepine ring.¹² The structural support came from an X-ray crystallographic analysis of the same type of TCNE adduct which was obtained from the photolysis of 2-azidobiphenyl in the presence of TCNE and showed a similar characteristic ¹H NMR signal at δ 8.49. The structure in this case proved to be 4-aza-2,2,3,3-tetracyano-9-phenylspiro[2.6]nona-4,6,8-triene.

Products **14** and **15** were obtained in the photolysis of **2** in a diethylamine solution. Azepine derivative **4** was not detected under these conditions. It is well established that the photolysis of phenyl azide derivatives in the presence of diethylamine gives 2-(diethylamino)-3*H*-azepine derivatives by the external capture of azirine and/or azacycloheptatetraene derivative **17**.¹³ In the present case, a primary photoproduct 2-(diethylamino)-3-(9-fluorenyl)-3*H*-azepine seems to have been autoxidized to give 2-(diethylamino)-3-(9-fluorenylidene)-3*H*-azepine (**14**). The ¹H NMR spectrum of the diethylamino group of **14** shows a characteristic pattern. Namely, two sets of methyl triplet signals at δ 0.92 and 1.34 and a complex methylene signal are observed. This indicates that the diethyl moiety is nonequivalent due to the partial double bond character of the C₂(sp²)-N(Et)₂ bond. Furthermore, methylene protons of each ethyl group are diastereotopic and give two sets of double quartet because of the distortion from the planarity between five- and seven-membered rings. Irradiation of the triplet signal at higher field (δ 0.92) changed one of the methylene signals to an AB quartet (δ 3.04, 3.18, 3.48, 3.64 (J = 13 Hz)), leaving the other as a double quartet. Meanwhile, irradiation of a triplet at lower field (δ 1.34) changes the other methylene signals to an AB quartet (δ 3.38, 3.53, 3.65, 3.79 (J = 13 Hz)). Formation of pyridine derivative **15** could be explained by the oxidative ring contraction of 1*H*-azepine derivative **12**, losing a carbon atom at the 5 position as formaldehyde. Both products are consistent with Sundberg's scheme for *o*-alkyl-substituted aryl azides.¹³

(c) **Difference in Reactivity of *ap*- and *sp*-*o*-(9-Fluorenyl)phenylnitrenes at Ambient and Cryogenic Temperatures.** One of the possible reasons for the slightly different product distributions in the photolysis of **1** and **2** would be the presence of two different conformers, *ap* and *sp* forms of *o*-(9-fluorenyl)phenylnitrene (**3a** and **b**). Photolyses of **1** and **2** were carried out in rigid glasses at cryogenic temperatures and monitored by UV absorption spectroscopy.^{6b} While the singlet nitrene from **1** was found to add to a double bond of the fluorene ring to form azanorcaradiene (**11**) (λ_{\max} 340 nm), in competition with intersystem crossing, the singlet nitrene from **2** isomerized to the *o*-quinoid-type tautomer **Q**. This difference in the behavior of the singlet nitrenes from

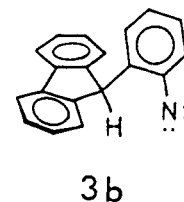
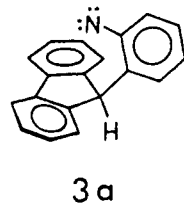


1 and **2** could be explained as follows: *ap* rotamer **3a** is formed from **1** by the least motion principle whereas *sp* rotamer **3b** is

(12) The NMR spectrum of compound **13** has a characteristic doublet (δ 8.34, J = 2 Hz) due to coupling with the methine proton at position 7 of the azepine ring. To the best of our knowledge, this type of compound has not been reported. Generality of formation of this kind of TCNE adducts was tested on phenyl azide, 2-methylphenyl azide, 2,4-dimethylphenyl azide, 2-*tert*-butylphenyl azide, and *o*-azidobiphenyl. All of them gave the same type of adducts as indicated by their ¹H NMR spectra at δ 8.3–8.5, but most of them were unstable and decomposed during the purification procedure. An X-ray crystal structure analysis was successful on the product of *o*-azidobiphenyl with TCNE (Murata, S.; Sugawara, T.; Iwamura, H. *J. Chem. Soc., Chem. Commun.* **1984**, 1198).

(13) Sundberg, R. J.; Suter, S. R.; Brenner, M. *J. Am. Chem. Soc.* **1972**, *94*, 513.

generated predominantly from **2** with conservation of the conformation. A conformational analysis of a chloroform-*d* solution of **2** by low-temperature ¹H and ¹³C NMR revealed that the equilibrium ratio of *sp/ap* was \geq 20:1.^{4f} The barrier to rotation around the bond between the phenyl and fluorenyl groups in *o*-(9-fluorenyl)aniline was found to be 13.6 kcal/mol,^{4f} and this value may approximate that for **3**, leaving no doubt that conformational interconversion between **3a** and **3b** should not occur at cryogenic temperatures.¹⁴



The sequence of steps in the addition of *ap*-nitrene **3a** to the double bond of the fluorene ring has been elucidated by time-resolved spectroscopy at ambient temperature.^{6b} A dual exponential rise curve for formation of **11** was interpreted as the intermediacy of a valence tautomer, azirine, and/or the azacycloheptatetraene derivative **17**, during the addition of **3a**. The higher yield of azepine derivatives **4** and **5** from **1** is reasonably understood on the basis of the *ap* conformation of the initially formed nitrene **3a** from **1**. Although the addition to the fluorene ring is not possible for the singlet nitrene **3b** for steric reasons, azepine derivatives **4** and **5** were also formed from azide **2** in yields higher than expected from the residual *ap* conformers. A conformational change from *sp* to *ap* forms during the photolysis has to be taken into account. A hint as to a possible mechanism for the facile formation of **4** and **5** from **2** is obtained from byproducts **13**, **14**, and **15** of the photolysis of **2** in the presence of TCNE or diethylamine. These products suggest the important contribution of azirine and/or azacycloheptatetraene intermediate **17**, especially in the photolysis of **2**.¹⁵ Since the lifetime of valence isomer **17** may be long enough to compete with rotation to convert *sp*-azacycloheptatetraene (*sp*-ACHTE (**17b**)) to *ap*-ACHTE (**17a**) and the resulting *ap*-ACHTE may regenerate *ap*-nitrene **3a**, the latter could add to the fluorene ring to give **5**. The rate of the conformational interconversion on **3** is estimated to be 2×10^3 s⁻¹ at 25 °C, assuming a barrier of 13 kcal/mol, while the rate of rotation in **17** should be much faster than this. On the other hand, the dual rate of the addition of the singlet nitrene **3a** was found by time-resolved spectroscopy to be $k_a = 4 \times 10^6$ s⁻¹ and $k_b = 1.0 \times 10^6$ s⁻¹.^{6b} Therefore, if the rate of bond rotation in **17** is much faster by two or three orders of magnitude, it would become comparable to that of the reaction.

The relative yields of azepine-TCNE adducts **5** and **13** were examined at several temperatures from 25 to -40 °C. While only **5** was obtained from **1** and its yield was practically the same at various temperatures, the yield of **13** from **2** increased considerably at the expense of **5** at lower temperatures (see run 6 in Table I). The tendency may be rationalized by the slower rotation around the C₉-ACHTE bond, giving higher chance of trapping of *sp*-ACHTE to form **13** at low temperatures (Scheme II).

We note that **17b** generated from **2** was also trapped externally by diethylamine. The amine was effective only as a base to promote isomerization of **12** to **4** in the photolysis of **1**. Since the *ap*-nitrene **3a** and/or *ap*-ACHTE **17a** has an efficient route for addition to the fluorene ring, the external trapping of **17a** could not compete (Scheme II).

The triplet nitrene **3** which is formed from singlet **3** through intersystem crossing should be able to add to a double bond of

(14) Significant differences in the chemical and spectroscopic properties between *ap*- and *sp*-nitrenes **3a** and **3b** were demonstrated by conformationally fixed azides, *ap*- and *sp*-3,5-dimethyl-2-(9-fluorenyl)phenyl azides. Murata, S.; Sugawara, T.; Iwamura, H. *J. Am. Chem. Soc.* **1983**, *105*, 3723.

(15) (a) Chapman, O. L.; Sheridan, R. S.; LeRoux, J. P. *J. Am. Chem. Soc.* **1978**, *100*, 6245. (b) Dunkin, I. R.; Thomson, P. C. P. *J. Chem. Soc., Chem. Commun.* **1980**, 499.

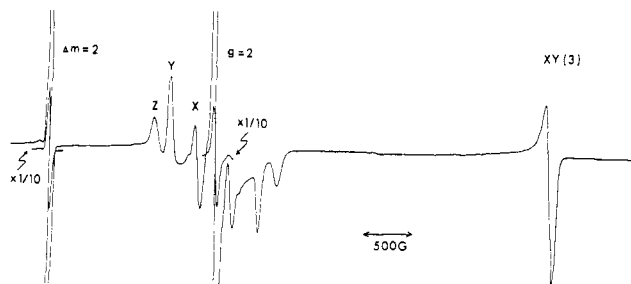
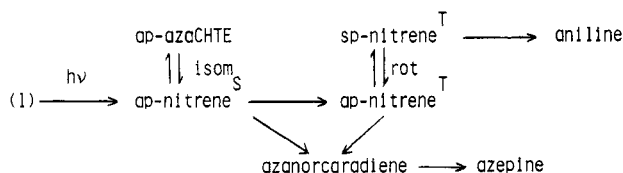
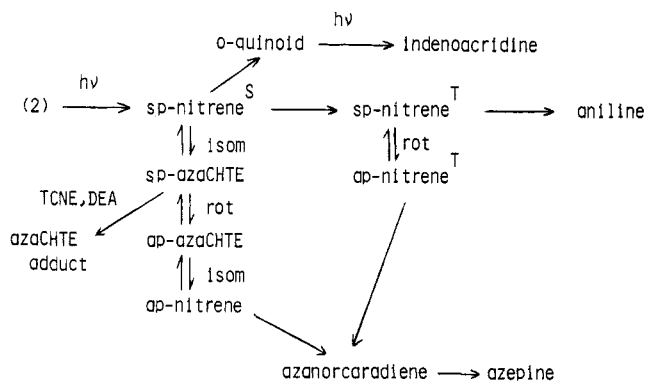


Figure 4. EPR spectrum obtained after irradiation of **1** in methylcyclohexane glass at 4.2 K. The klystron frequency was 9.30 GHz. In addition to the X,Y transition due to triplet **3**, there is a strong signal at $g = 2$ due to the adventitious formation of free radicals. The remaining signals are assigned to diradical **18**, accompanied by $\Delta m = 2$ transition.

Scheme II



the fluorene ring in the *ap* conformation as well.¹⁶ Since the lifetime of the triplet nitrene is relatively long (10^{-3} s), bond rotation in the triplet nitrene can compete with its reactivity. It is thus not surprising to obtain the same azepine compounds from *ap* and *sp* triplet nitrenes.¹⁶ Formation of aniline derivative **16** in the photolysis at cryogenic temperatures indicates that the abstraction reaction is a competing process.

(d) Detection of the Triplet *o*-(9-Fluorenyl)phenylnitrene by ESR. Irradiation of **1** with a low-pressure mercury lamp in methylcyclohexane glass at 4.2 K produced an intense signal at 6730 G in the X-band ESR spectrum. The signal is assigned to the characteristic X,Y transition of triplet *o*-(9-fluorenyl)phenylnitrene **3** ($D = 1.0 \text{ cm}^{-1}$, $E = 0.0 \text{ cm}^{-1}$), shifted to lower field by 94 G compared with that of the parent phenylnitrene. No signal due to a phenylcarbene derivative was detected, providing independent evidence against the possibility of extrusion of the bridgehead carbon atom. The nitrene was independently generated by the photolysis of *o*-(9-fluorenyl)phenyl azide (**2**). The observed X,Y transition at 6750 G was very similar to that obtained from **1**, but the field position was 20 G higher in the case of **2** (see Figures 4 and 5). This slight but meaningful difference is ascribed to the different conformations of the nitrene **3**; *ap* rotamer **3a** was formed from **1**, whereas *sp* rotamer **3b** was predominantly generated from **2** on the heavy bias because the

(16) In the case of photorearrangement of triptycene, both the singlet and triplet states are shown by the xenon perturbation technique to be responsible for the formation of the norcaradiene product in a ratio of $\geq 5:1$. Tukada, H.; Iwamura, H., to be published.

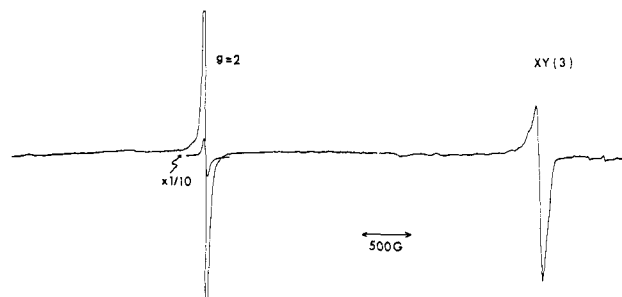


Figure 5. EPR spectrum obtained by photolysis of **2** in methylcyclohexane glass at 4.2 K.

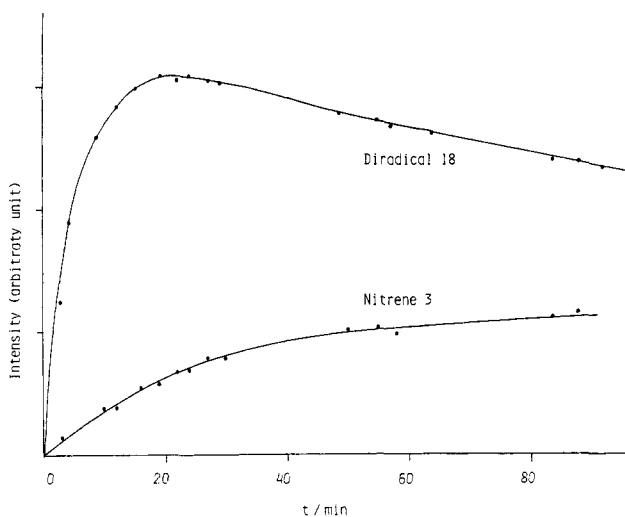
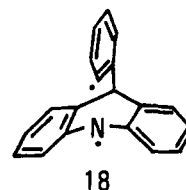


Figure 6. Growth curves of the triplet signals during irradiation of 1-azatriptycene in methylcyclohexane (4.27×10^{-4} M) at 4.7 K.

conformational equilibrium was shifted to the *sp* form in **2** as discussed before.

The lower resonance field of **3a** from **1** suggests that one of the *p* electrons on the univalent nitrogen may be more delocalized in **3a** than in **3b**.¹⁷ This can be rationalized by assuming through-space interaction in **3a** between the closely located fluorene ring and the univalent nitrogen.¹⁴

In addition to the nitrene signal, a pair of multiplets was observed in the $g = 2$ region ($D = 0.060 \text{ cm}^{-1}$; $E = 0.0083 \text{ cm}^{-1}$), accompanied by a $\Delta m = 2$ transition at 1670 G. These signals are characteristic of a triplet diradical. Since the zero-field parameter for the triplet state of triptycene is reported to be $D = 0.135 \text{ cm}^{-1}$ and the signals showed a temperature dependence,¹⁸ the triplet state of 1-azatriptycene (**1**) was excluded as a candidate for the observed triplet signal. The most conceivable diradical is the one formed by the one-bond fission of the *N*-phenyl bond to give **18**. The species corresponds to the intermediate which



Wittig and Steinberg proposed hypothetically.⁹ Assuming the point dipole approximation, the average distance between the unpaired electrons was estimated to be 3.5 Å. The distance suggests the diradical may not be fully relaxed geometrically but preserving a structure which is still close to reactant geometry.

The genetic correlation between the nitrene and the diradical was also investigated. The growth curves of nitrene **3a** and triplet

(17) Hall, J. H.; Fargher, J. M.; Gislis, M. R. *J. Am. Chem. Soc.* **1978**, *100*, 2029.

(18) De Groot, M. S.; van der Waals, J. H. *Mol. Phys.* **1963**, *6*, 545.

species **18** are shown in Figure 6. Both **3a** and **18** rose immediately after the start of irradiation and no tendency was observed for one to be the precursor of the other. The diradical was found to be unstable and decayed with a half-life of 18 min at 45 K, while the intensity of **3a** remained constant during the decay of the diradical in the dark (Figure 7). The decay of diradical **18** obeyed strictly first-order kinetics, which suggests that the decay process is a recombination of the diradical to regenerate **1**. If the decay process were abstraction of hydrogen from the surrounding molecules, the decay kinetics should have deviated from a first-order plot due to the inhomogeneous distribution of hydrogen atoms to be transferred from matrices.

Irradiation of the accumulated **3a** and **18** with longer wavelength light than 400 nm caused a rapid decay of both species. These results clearly show that no thermal or photochemical interconversion exists between **3a** and **18** but that the two species are generated independently.

The irradiation product of **1** at cryogenic temperature was revealed by HPLC to contain a small amount of the indenoacridine. This may presumably be formed by the Wittig mechanism of diradical **18**, since irradiation of **1** in methanol at ambient temperature did not give 9-phenylacridine, its 9,10-dihydro derivative, or indeno[*k*l]acridine. The results suggest that the one C-N bond cleavage process is minor and negligible at room temperature due to the smaller enthalpy of activation of the process.

(e) **Mechanistic Details of the Primary Processes of the 1-Azatriptycene Photorearrangement.** (1) **Diversion from Di- π -methane Rearrangement and Bridging Regioselectivity.** It is interesting to discuss the unique reactivity of triptycenes in reference to those of barrelene and its mono and dibenzo derivatives. If photochemistry of **1** were to be in parallel with that of barrelene and its derivatives,⁵ direct irradiation would have given a product resulting from intramolecular 2 + 2 cycloaddition followed by retro-Diels-Alder opening or an anti-Bredt olefin (**19**) with the destruction of one of the benzene rings. Sensitized photolysis should have given a biradical intermediate (**20**) with the loss of the resonance energy of two benzene rings. Neither of them appears to be an energetically favorable route; and photorearrangement of **1** does proceed through an extrusion mechanism instead. The unique reactivity of the triptycenes may also be ascribed to the relatively high p character of the C-C bonds at the bridgehead and strain energy of the triptycene skeleton.¹⁹ Thus, the nitrene is formed directly from the excited singlet state of **1** through a cheletropic reaction.



Quantum yields of the photoreaction were determined on triptycenes based on the consumption of the substrate in various solvents. While the quantum yields were roughly constant ($\Phi_r \sim 0.3$) for triptycenes, those for 1-azatriptycene varied from 0.44 to 0.66 as the polarity of the solvent increased (Table IV). The difference may be ascribed to the presence of the heteroatom in **1**, suggesting the polar effect in the transition state of the photoextrusion reaction.

Several factors might be responsible for the observed bridging selectivity displayed in formation of a nitrene rather than a carbene from **1**. The first point along the reaction coordinate of the di- π -methane rearrangement would be the geometrical nonequivalence of the two ends of the *o*-benzene moieties in this rather rigid molecule. The C-N bond distance is expected to be ca. 1.45 Å (1.45 Å for trimethylamine and 1.46 Å for 1-aza-6-phospha-

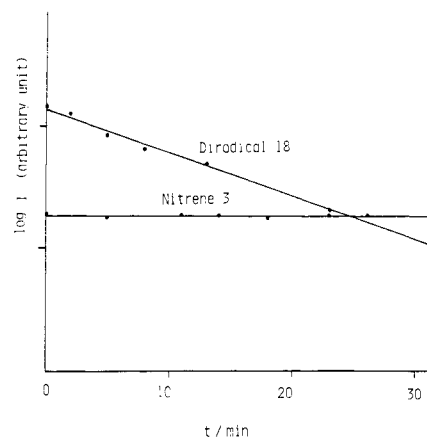


Figure 7. Decay plots of the signal intensities due to diradical **18** at 45 K in the dark.

Table IV. Quantum Yields of Photorearrangement of 1-Azatriptycene (**1**)

solvent ^a	ϕ_r^b
cyclohexane	0.44 ± 0.03
methanol	0.57 ± 0.03
acetonitrile	0.66 ± 0.01

^a C = 0.99 ~ 1.49 × 10⁻⁴ M. ^b At 270 ± 5 nm at 25.0 °C.

triptycene) and should be decidedly shorter than the 1.53 Å observed for the bridgehead-to-benzene C-C bonds in many triptycenes.²⁰ Therefore, the distance between the two benzene rings is shorter and π - π overlap can be more effective at the end near the nitrogen bridgehead.

In order to understand the bridging selectivity of **1** more quantitatively, a semiempirical MO calculation (MINDO/3) was carried out on 1-azabarrelene as a model system. There are two degenerate LUMO's which have antibonding character within each ethylene moiety but have bonding character between ethylene moieties at the nitrogen and carbon ends, respectively. Besides the slightly shorter distances between the aromatic carbon atoms at the nitrogen end, the coefficient of the p_π orbitals on the carbon atoms attached to the bridgehead atoms is 4% larger at the nitrogen end. These characteristics rationalize the favorable bonding at the nitrogen end in the photoexcited state of the 1-azabarrelene skeleton. Higher electronegativity of nitrogen vs. carbon may be employed to rationalize the higher stability of the initially formed aziridine-2,3-dicarbonyl diradical as compared to cyclopropyl-dicarbonyl diradical. Rationalization for this argument is based on the inductive effect of a heteroatom on strengthening the opposite C-C bond of the three-membered ring and is supported by the findings on the effect of the heteroatom on the equilibrium of the tropilidene-norcaradiene valence tautomerization. The norcaradiene structure becomes more stabilized as we go from CH₂ through NH to O at position 7.²¹ If the next step of rearrangement of the initially formed diradicals can be product controlling, or the second step takes place concertedly with the first bridging, the weaker C-N bond energy relative to the C-C would be invoked. Conclusions on these points must be postponed until a more systematic study on the effect of substituents at the "methane" position on the bridging regioselectivity is completed.

(2) **The Excited State of Triptycenes.** Absorption and fluorescence spectra of 1-azatriptycene and triptycene were measured in order to fully characterize the excited singlet state from which monocentric biradical species, namely, a nitrene or a carbene, are generated in high efficiency. Interest in the nature of the triply degenerate chromophoric system in triptycenes has attracted a number of studies. These include the ingenuous argument on the enhanced UV absorptivity,^{3a} the exciton theory

(19) The NMR coupling constant between the bridgehead carbon and methine proton is $J(^{13}\text{C}-\text{H}) = 141.5$ Hz, indicating the $sp^{2.4}$ hybridization of the bridgehead carbon-to-hydrogen bond.

(20) Anzenhofer, K.; de Bohr, J. J. *Z. Kristallogr.* **1970**, *131*, 103.

(21) (a) Stoher, W.-D. *Chem. Ber.* **1973**, *106*, 970. (b) Günther, H.; Pawliczek, J. B.; Tunggal, B. D.; Prinzbach, H.; Levin, R. H. *Chem. Ber.* **1973**, *106*, 984.

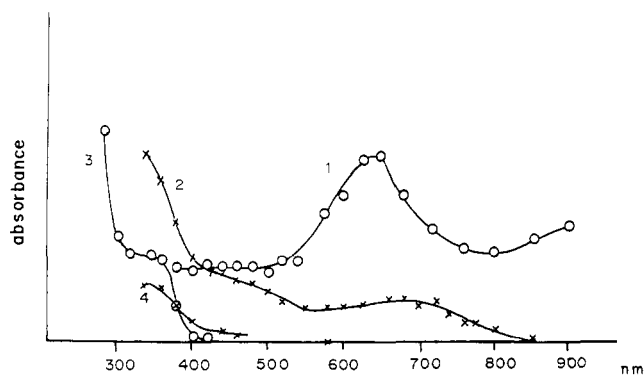


Figure 8. Time-resolved absorption spectra of triptycene (O) (5.3×10^{-4} M) and *o*-xylene (X) (1.6×10^{-3} M) in cyclohexane at 16.5 °C: 1 and 2, at the peak of the time trace ($S_n \leftarrow S_1$ spectra); 3, after 200 ns (photoproduct of triptycene);⁴ and 4, after 200 ns ($T_n \leftarrow T_1$ spectrum).

on the CD spectra of chiral triptycene molecules,^{3c} and the ESR observation of the triplet exciton at 77 K.¹⁸

The two lowest excited states of triptycene (symmetry D_{3h}) can be expressed as follows, on the basis of an exciton model, the ground-state functions and excited-state ones of benzenoid moieties being a , b , c and a^* , b^* , c^* , respectively.

$$\Psi(A_2'') = 3^{-1/2}(a^*bc + ab^*c + abc^*)$$

$$\Psi(E') = 2^{-1/2}(a^*bc - ab^*c)$$

$$\Psi(E'') = 6^{-1/2}(a^*bc + ab^*c - 2abc^*)$$

Absorption spectra of a cyclohexane solution of 1-azatriptycene and triptycene show a benzenoid ${}^1B_{2u}$ transition at 264, 271, 278 nm, having vibrational structures with a spacing of 950 cm^{-1} . The band of **1** is superimposable on that of triptycene, indicating no perturbation of the nitrogen lone pair to the ${}^1B_{2u}$ transition because of the perpendicular orientation of the lone-pair electrons to π orbitals of the benzene rings. Absorption maxima showed a bathochromic shift of 7 nm and enhanced absorptivity when compared with *o*-xylene as a reference compound (the ratio of integrated intensities of ${}^1B_{2u}$ of triptycenes to that of *o*-xylene is 7 or 2.3 per ring). Although Bartlett et al. pointed out that a charge-transfer interaction would be important in the S_1 state to explain these spectral features of triptycene, the tendency may reasonably be explained by the argument that the intensity of the ${}^1B_{2u}$ transition of one benzene ring becomes stronger by borrowing intensity from the ${}^1E_{1u}$ transition of the other two benzene rings. In terms of the D_{3h} symmetry of the triptycene molecule, this band corresponds to the dipole-allowed ${}^1E' \leftarrow 1A_1'$ transition.

The $S_n \leftarrow S_1$ absorption spectrum of triptycene has now been measured in cyclohexane solution by nanosecond laser spectroscopy, using a KrF excimer laser.^{1d} The sample solution was renewed at every pulse to remove the effect of the photoproducts on the spectrum. Peak transient absorption spectra of triptycene and *o*-xylene are reproduced in Figure 8. The spectrum of triptycene extended out to 900 nm, showing a tremendous bathochromic shift and enhanced absorptivity compared with that of *o*-xylene.

Although the fluorescence lifetime of *o*-xylene is 34 ns, that of triptycene is only 2.4 ns, which is shorter than the laser pulse width of 15 ns, resulting in underestimation of the intensity of the $S_n \leftarrow S_1$ spectrum of triptycene. Even before intensity correction, the extinction coefficient of the 650-nm band of triptycene is larger than that of *o*-xylene. The band of the latter, at 680 nm, corresponds to the vibrationally allowed ${}^1E_{1u} \leftarrow {}^1B_{1u}$ transition of benzene, for which the extinction coefficient is estimated to be 410 .^{1d} In order to obtain information on the character of this transition in triptycene, the extinction coefficient was estimated by deconvoluting the pulse shape of the absorption at 650 nm, assuming a Gaussian shape for the laser pulse. The ratio of coefficients $R = \epsilon_{650}^{\text{Triptycene}} / \epsilon_{680}^{\text{o-xylene}}$ was calculated to be 180, which allowed us to estimate the extinction coefficient of triptycene to be $7400\text{ M}^{-1}\text{ cm}^{-1}$ as a minimum value, assuming the extinction

Table V. Quantum Yields of Fluorescence of Triptycene and 1-Azatriptycene

solvent ^a	$\phi_f(\text{triptycene})^b$	$\phi_f(1\text{-azatriptycene})^b$
cyclohexane	0.30	0.10
methanol	0.35	0.13
acetonitrile	0.33	0.14

^a $C = 0.896 \pm 1.38 \times 10^{-4}$ M. ^b Excitation at 254 nm at 298 K.

coefficient of *o*-xylene is 410 (this is the lowest estimate for *o*-xylene). This value corresponds to an oscillator strength of 0.85, which indicates that the transition is an allowed one. The region of the peak at 650 nm corresponds to the weak ${}^1E_{1u} \leftarrow {}^1B_{2u}$ transition (λ_{max} 620–700 nm) in dilute solution for benzene and *o*-xylene (10^{-3} M).^{1d} A strong absorption was detected at 500 nm in concentrated solution (10^{-1} M) for benzene, and this was assigned to the absorption of an *intermolecular* excimer.^{1d} Therefore, the intense absorption at 650 nm of a dilute solution of triptycene may be assigned to that of the *intramolecular* excimer between the benzenoid moieties of the triptycene molecule. Although mutual orientation of the benzenoid chromophores in triptycenes is apparently unfavorable for the excimer type of interaction, a geometric change in the excited state coupled with some vibrational modes could make the interaction effective via through-space and/or through-bond mechanisms.²² It is well demonstrated from fluorescence behavior of arylethylenes or dianthryl that torsional vibrations with a large amplitude can be frozen out in rigid glasses.²³ Therefore, the $S_n \leftarrow S_1$ spectrum of triptycene was recorded in a rigid isopentane glass at 77 K in order to freeze out any geometrical change of the triptycene skeleton in the excited state. The CT transition at 650 nm did not disappear but decreased slightly in intensity which is consistent with the above interpretation.

After disappearance of the $S_n \leftarrow S_1$ spectrum ($\tau_f = 2.4$ ns), absorptions due to the norcaradiene product developed. Unlike benzene, *o*-xylene, and [2.2]paracyclophane, triptycene did not give a $T_n \leftarrow T_1$ spectrum, which suggests that norcaradiene was formed predominantly from the excited singlet state. The xenon perturbation¹⁶ method shows that more than 80% of the norcaradiene derivative comes from the singlet state of triptycene, which is independent evidence for the above conclusion. While quantum yields of fluorescence and reaction are high, $\Phi_f = 0.30$ (in methanol) and $\Phi_f = 0.48$ (in cyclohexane), that of phosphorescence is practically zero in hydrocarbon glass at 77 K ($\Phi_p < 0.01$).

In order to examine the interaction between the benzenoid chromophores of triptycenes, the fluorescence behavior was investigated. The fluorescence lifetime was found to be 2.4 ns in methanol at ambient temperature and 4.2 ns at 77 K. Quantum yields of fluorescence of triptycenes in various solvents were determined by using *o*-xylene as a reference compound. As shown in Table V, the quantum yield is lower for **1** compared with triptycene and neither of them showed dependence on the solvent polarity. The relatively short τ_f and not very high Φ_f ($=0.1$) reflect the high Φ_f of **1**. Fluorescence of **1** was quenched both by diethylamine and tetracyanoethylene. From the Stern–Volmer plots, the quenching rate constants in acetonitrile solution were obtained as $k_q = 4.1 \times 10^9\text{ L mol}^{-1}\text{ s}^{-1}$ for the amine²⁴ and $\sim 2 \times 10^{10}\text{ L mol}^{-1}\text{ s}^{-1}$ (practically diffusion controlled) for TCNE. The quantum yield of phosphorescence must be very small ($\Phi_p < 0.01$),

(22) In order to explain the CD spectra of chiral triptycene derivatives, homoconjugation of ca. 20% is postulated between two benzene rings.^{3c,d}

(23) (a) Stegemeyer, H. *Ber. Bunsenges. Phys. Chem.* **1968**, *72*, 335. (b) El-Bayoumi, M. A.; Halim, F. M. *J. Chem. Phys.* **1968**, *48*, 2536. (c) Birks, J. B. "Organic Molecular Photophysics"; Wiley: New York, 1975; Vol. 2, p 474.

(24) The fluorescence quenching of **1** with diethylamine is thought to take place through an electron-transfer mechanism. Triethylamine also serves as a quencher. The lack of self-quenching in **1** comes presumably from the expected higher ionization potential of the lone pair of electrons and the configurational rigidity at the nitrogen atom of **1**. The $k_q[Q]$ value in run 7 is now calculated to be $4 \times 10^9 \times 4 \times 10^{-4} = 1.6 \times 10^6\text{ s}^{-1}$ and sufficiently smaller than the unimolecular rate constant for the reaction ($k_f = 1.2 \times 10^8\text{ s}^{-1}$)^{6b} of **1**.

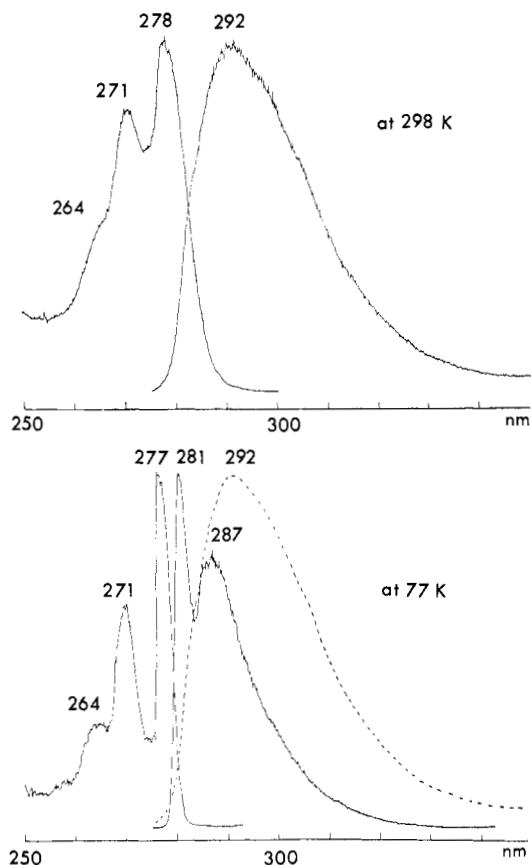


Figure 9. The fluorescence and excitation spectra of 1-azatriptycene (**1**) in 2,2-dimethylbutane/*n*-pentane (8:3, v/v) (2.3×10^{-4} M) at 298 and 77 K.

since phosphorescent emission could not be detected for triptycenes in glassy solvents at 77 K.²⁵

The fluorescence emission and excitation spectra of **1**, obtained in fluid solution at ambient temperature and in a 2,2-dimethylbutane-pentane (8:3, v/v) matrix at 77 K, are reproduced in Figure 9. The fluorescence at ambient temperature is characterized by a diffuse band having its maximum at 292 nm and extending to 340 nm. The spectrum did not show any concentration dependence down to 10^{-6} M. The fluorescence excitation spectrum is superimposable on the UV absorption not only of **1** but also of hydrocarbon triptycene, indicating the $\pi-\pi^*$ nature of the S_1 state. The peaks at 264, 271, and 278 nm in the excitation spectrum correspond to the vibrational structure with a progression of 950 cm^{-1} . In the hydrocarbon matrix at 77 K, the fluorescence is nearly a mirror image of the S_1 transition in the UV absorption spectrum, showing the well-resolved vibrational structure and having a sharp maximum at 281 nm. Since quite similar dependence of fluorescence on the temperature and/or medium is observed on triptycene itself, the following two possibilities are ruled out as an origin of the observed effect: effective reorientation of solvent molecules around the nitrogen atom of **1** in fluid solution and dual fluorescence of $n-\pi^*$ and $\pi-\pi^*$ states.

Time-resolved fluorescence measurements of **1** and triptycene were carried out in hydrocarbon solvent at ambient temperature. A broad structureless emission was obtained even 100 ps after the excitation, and Frank-Condon-type emission was not detected.²⁶ The result suggests that the torsional relaxation is on the order of one vibration, 10^{-13} s. Recently, fluorescence and excitation spectra of triptycene were successfully measured in a super-sonic jet.²⁷ Although the rotational temperature of trip-

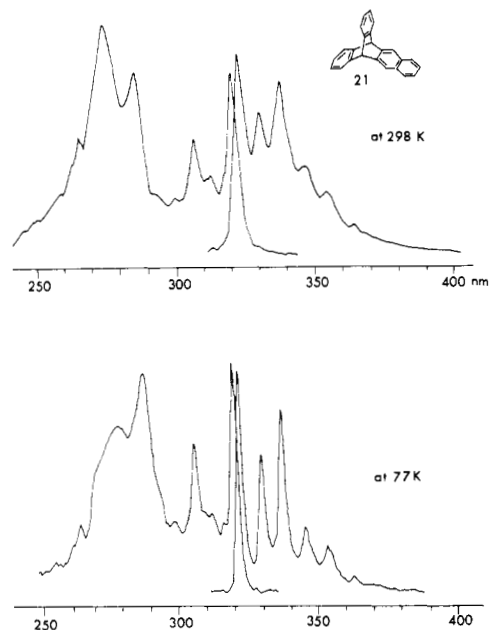


Figure 10. Fluorescence and excitation spectra of benzotriptycene **21** in isopentane (1.44×10^{-5} M) at 298 and 77 K.

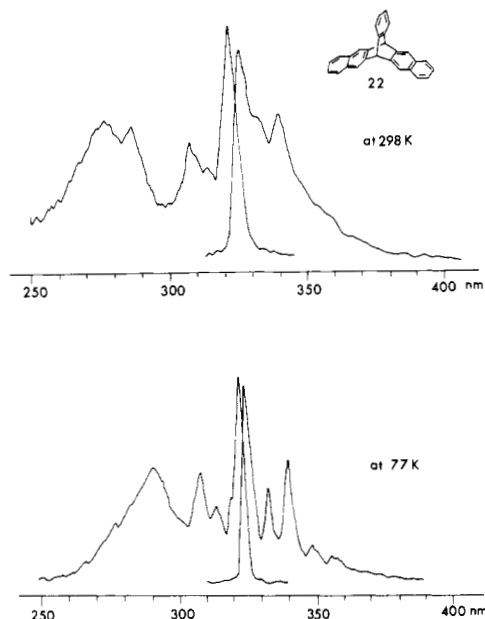


Figure 11. Fluorescence and excitation spectra of dibenzotriptycene **22** in isopentane (1.07×10^{-5} M) at 298 and 77 K.

tycene is as low as 2 K, the emission turned out to be broad and structureless. Therefore, the previous structured emission should be ascribed mainly to the high viscosity of rigid glasses.

In order to examine the structureless emission of the triptycene skeleton, fluorescence spectra of 5,12-dihydro-5,12-(*o*-benzeno)naphthacene (**21**) and 6,13-dihydro-6,13-(*o*-benzeno)pentacene (**22**)²⁸ were measured at ambient and cryogenic temperatures. The fluorescence spectrum of **21** showed a clear vibrational structure of a naphthalenoid moiety even at ambient temperature, and it became very sharp at 77 K in a rigid glass (Figure 10). This may indicate that the excitation energy is localized on a naphthalene chromophore in **21**. While the vibrational structure of **22** was very diffuse at ambient temperature, it became as sharp as **21** at 77 K in a rigid medium (Figure 11). The tendency may be rationalized by the excitonic interaction

(25) This is in conflict with the preliminary report by Turro et al.^{4b}

(26) Experimental apparatus and procedures are the same as described in the following literature. (a) Murao, T.; Yamazaki, I.; Yoshihara, K. *J. Spectrosc. Soc. Jpn.* **1982**, *31*, 96. (b) Yamazaki, I.; Murao, T.; Yoshihara, K. *Chem. Phys. Lett.* **1982**, *87*, 384.

(27) Bersohn, R.; Even, U.; Jortner, J. *J. Chem. Phys.* **1983**, *79*, 2163.

(28) Compounds **21** and **22** were prepared according to the literature method. Godfrey, R. *J. Chem. Soc., Perkin Trans. 2* **1978**, 1019.

between the two degenerate chromophores in **22** (a weak interaction case, where the interaction energy is comparable to the Frank-Condon bandwidth). However, the excitonic energy becomes localized at 77 K by freezing out vibrational modes. Jortner et al. proposed, based on a well-resolved excitation spectrum obtained by a super-sonic jet,²⁷ that low-energy vibrational modes (50–120 cm⁻¹) may correspond to the degenerate torsion around the molecular threefold axis and that if vibrational energy accumulates in this particular mode and exceeds the threshold value the isomerization of triptycenes may take place.

Therefore, the fluorescence behavior of **1** and triptycene should be interpreted as follows: excitonic coupling through vibrational modes makes the vibrational structure diffuse in fluid solution or in an isolated molecule in the gas phase, but it can be largely frozen out in rigid media. In other words, *C*_{3v} symmetry of **1** could be maintained in the Frank-Condon state in the rigid media, but the symmetry may be lower in the two fluid states. The suggested S₁ state structure in the fluid medium would be described as having deformed already along the reaction coordinate toward the photoproduct.²⁹

Lastly, it is intriguing to compare interactions between the benzene rings in the excited states and the consequent reactivity of triptycenes with those of [2.2]paracyclophane (CP) in the light of the different modes of overlapping of benzene moieties. The absorption spectrum of CP exhibits a charge-transfer band extending to 340 nm as well as local excitation bands.² Photoreaction takes place effectively by irradiation at the latter bands and proceeds via the excited triplet state reached by two photons, affording ethylenebis(benzyl) diradicals. In sharp contrast with this, photorearrangement of triptycenes proceeds through the excited singlet state by one photon, affording a monocentric biradical species with the bonding between two benzene rings. The contrasting reactivity should be ascribed to the different geometrical framework accompanied by the different modes of interaction in the excited states of the molecule.

Conclusion

Even though a variety of photoproducts are obtained depending on the reaction conditions, photochemistry of 1-azatriptycene is concluded to proceed through *ap*-2-(9-fluorenyl)phenylnitrene. On the contrary, it is the *sp*-nitrene which is formed by photolysis of 2-(9-fluorenyl)phenyl azide. The different conformations of the nitrene intermediate are responsible for the subtle change in the reactivity and the UV and ESR spectroscopic properties of these two precursors. The contrasting behavior provides a good lesson that alternative precursors leading supposedly to a common intermediate have to be chosen with care in mechanistic studies. Photochemistry of triptycenes has been found to have the primary process in common. Namely, the fluorescent state from which the photorearrangement takes place is different from the Frank-Condon state and is already one step ahead toward the product on the excited-state reaction surface.

Experimental Section

General. Proton NMR spectra were recorded on Varian EM-390 (90 MHz), JEOL FX 100 (99.55 MHz), and Bruker WM-360 (360 MHz) spectrometers. UV and fluorescence spectra were recorded on Cary 17 and Shimadzu RF-502 spectrometers, respectively. Microanalyses were performed either at the Microanalysis Center of Wako Pure Co. Ltd. or the Elemental Analysis Center of the Department of Chemistry, Faculty of Science, the University of Tokyo. Melting points were determined by use of a Laboratory Device Mel-Temp melting point apparatus and are uncorrected. For analytical high-performance liquid chromatography, a Waters Model ALC/GPC 244 apparatus equipped with a μ -Bondapak C₁₈ column (1/4 in. \times 1 ft) was used with methanol-water (4:1 v/v

unless otherwise stated) with a flow rate of 1.0 mL/min of the eluent. For preparative chromatography, a Japan Analytical Industry Co., Ltd. Model IC-09 apparatus was used with a series of JAIGEL 1H and 2H columns and a flow of 3 mL/min of chloroform (a gel permeation mode). LiChroprep Si 60 (Merck, size B) were used, if necessary, in conjunction with a Duramat pump and an Altex UV detector.

Materials. Methanol, acetonitrile, and diethylamine were purchased from Wako Pure Chemical Industries, Ltd. (extra pure grade) and distilled before use.

1-Azatriptycene (**1**), indenoacridine (**9**), 9-phenylacridine, and 9,10-dihydrophenylacridine were prepared according to literature methods.⁹ Preparations of *o*-(9-fluorenyl)aniline (**16**) and *o*-(9-fluorenyl)phenyl azide (**3**) were described in the previous paper.^{6b}

General Procedure for Preparative Photolysis. A solution of 100 mg (0.39 mmol) of **1** or **2** in 300 mL of methanol in the presence or absence of the additives was irradiated with a 14W low-pressure mercury lamp in an immersion apparatus under a bubbling atmosphere of nitrogen. The progress of the reaction was monitored by analysis of aliquots with HPLC: After the 60–70% conversion, the irradiation was stopped and the solvent was removed under reduced pressure. The crude reaction mixture was subjected to gel permeation chromatography (GPC) followed, if necessary, by silica gel chromatography on LiChroprep Si 60 (Merck, size B). Irradiation at –40 °C was carried out by immersing the whole photochemical vessel into a circulating isopropyl alcohol bath (CryoCool CC-100 Neslab Instruments, Inc.).

Photolysis of 1 in Methanol in the Presence of Sodium Methoxide (Run 1). A solution of 107 mg (0.42 mmol) of **1** in 300 mL of methanol containing sodium methoxide (1.3 mmol) was irradiated for 3 h. The mixture was separated by GPC to give two peaks at 63 min (minor) and 64 min (major) with a flow rate of 3.6 mL/min. Recrystallization of the major fraction from methanol-ether (1:1) gave 48 mg (68% based on the 66% conversion of **1**) of **4**: orange needles; mp 162–164 °C dec; ¹H NMR (CDCl₃) δ 3.80 (2 H, t-like, *J* = 4.5, 4.2 Hz), 4.71 (1 H, dt, *J* = 10 Hz, 4.5 Hz), 6.32 (1 H, t, *J* = 4.2 Hz), 6.73 (1 H, d, *J* = 10 Hz), 7.0–7.8 (8 H, m); UV (cyclohexane) λ_{max} 249 (log ϵ 4.73), 259 [sh] (4.63), 273 (4.53), 340 (3.37), 355 (3.50), 374 (3.43), 405 nm (3.16); mass spectrum M⁺ 255 (100%).

Anal. Calcd for C₁₉H₁₃N: C, 89.38; H, 5.13; N, 5.49. Found: C, 89.58; H, 5.08; N, 5.60.

The minor product, 8 mg of azepinone derivative **7**, was obtained in 7% yield as purple needles: mp 288 °C dec; ¹H NMR (CD₂Cl₂) δ 6.18 (1 H, dd, *J* = 10.0 Hz, 1.9 Hz), 7.20 (1 H, d, *J* = 1.9 Hz), 7.85 (1 H, d, *J* = 10.0 Hz), 7.25–7.92 (8 H, m); ¹³C NMR (CDCl₃) δ 187.8 (C=O); IR (Nujol) 1635, 1600 cm⁻¹; mass spectrum M⁺ – 269 (78.1%), M⁺ – CO 241 (100%), *m/e* 110 (80%); calcd for C₁₉H₁₁NO 269.0841, found 269.0854.

Azepinium Salt 6. A solution of 26.5 mg (0.104 mmol) of **4** in 4 mL of diethyl ether was added to a solution of trityl tetrafluoroborate (33 mg, 0.1 mmol) in 12 mL of chloroform at 0 °C. The mixture was stirred for 10 min to give a precipitate, which was filtered and washed with chloroform. The crude salt was recrystallized from ether:acetonitrile (1:1 v/v) to give dark brown solids: ¹H NMR (CD₃CN) δ 7.70 (1 H, t, *J* = 8.0 Hz), 7.96 (1 H, t, *J* = 8.1 Hz), 8.10 (1 H, t, *J* = 8.0 Hz), 8.16 (1 H, d, *J* = 8.0 Hz), 8.25 (1 H, dd, *J* = 11.8, 7.9 Hz), 8.39 (1 H, d, *J* = 8.0 Hz), 8.53 (1 H, d, *J* = 8.1 Hz), 8.72 (1 H, d, *J* = 8.4 Hz), 8.89 (1 H, d, *J* = 8.8 Hz), 9.15 (1 H, dd, *J* = 11.8, 8.8 Hz), 10.26 (1 H, d, *J* = 7.9 Hz).

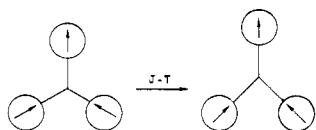
Photolysis of 1 in Acetonitrile in the Presence of TCNE (Run 3). A solution of 100 mg (0.39 mmol) of **1** and 100 mg (0.78 mmol) of TCNE in 300 mL of acetonitrile was irradiated for 2 h. The TCNE adduct **5** was obtained (81 mg) in 74% yield based on the reacted **1** and was purified by GPC (52 min) and recrystallized from *n*-hexane-benzene (1:1 v/v) to give white flakes: mp 183–5 °C dec; ¹H NMR (CDCl₃) δ 3.92 (1 H, m), 5.04 (1 H, dd, *J* = 8.2, 8.5 Hz), 5.24 (1 H, br s), 6.76 (1 H, dd, *J* = 8.2, 3.0 Hz), 7.02 (1 H, d, *J* = 6.6 Hz), 6.8–7.8 (8 H, m); mass spectrum M⁺ 383 (10.8%).

Anal. Calcd for C₂₃H₁₃N₅: C, 78.32; H, 3.41; N, 18.27. Found: C, 78.61; H, 3.15; N, 18.09.

A minor product, 5 mg (5%) of indenoacridine (**9**), was separated by GPC, purified by alumina column chromatography, and found to be identical with the authentic sample.⁹

Photolysis of 1 in Acetic Acid (Run 8). A solution of 287 mg (1.13 mmol) of **1** in 300 mL of acetic acid was irradiated. The progress of the reaction was monitored by HPLC. The retention times of **1**, *o*-(9-fluorenyl)aniline (**16**), dihydromethylindenoacridine (**10**), and indenoacridine (**9**) were 7.0, 7.9, 13.4, and 23.8 min, respectively, at the flow rate of 1 mL/min of methanol-water (3:1, v/v). The relative intensity of the components was calibrated to follow the change in the concentrations of the starting material and the products. After 16 h of irradiation, **10** was separated by GPC (*R*_t = 64 min) and recrystallized from

(29) This Jahn-Teller distortion makes the degenerate ¹E₁' states split and one of the states in which two chromophores are in phase is stabilized as a result of enhanced interaction



n-hexane-dichloromethane (1:1, v/v) to give 176 mg (58%) of white granules: mp 151–153 °C; ¹H NMR (CDCl₃) δ 1.40 (3 H, s), 6.30 (1 H, br s, disappeared on shaking with D₂O), 6.8–8.0 (11 H, m); IR (Nujol) 3370, 1580, 1290, and 740 cm⁻¹.

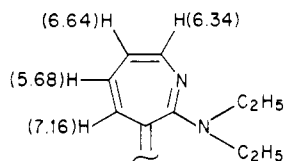
Anal. Calcd for C₂₀H₁₅N: C, 89.19; H, 5.61; N, 5.20. Found: C, 89.35; H, 5.54; N, 5.06.

Photolysis of 2 in Methanol in the Presence of Sodium Methoxide (Run 2). A solution of 110 mg (0.39 mmol) of azide 2 in 130 mL of methanol containing sodium methoxide (0.44 mmol) was irradiated for 30 min. The reaction mixture was separated by GPC to give 24 mg of 4 (34% based on the 72% conversion of 2).

Photolysis of 2 in Acetonitrile in the Presence of TCNE (Run 5). A solution of 111 mg (0.39 mmol) of 2 in 130 mL of acetonitrile was irradiated for 20 min. The reaction mixture was separated as in the case of 1 to give 72 mg (48% yield) of major product 5. The minor product (53 mg) was obtained as a pale yellow oil (23 mg, 16%): ¹H NMR (CDCl₃) δ 5.08 (1 H, s), 6.40 (1 H, d, *J* = 5 Hz), 6.98 (2 H, m), 7.1–8.0 (2 H, m), 8.34 (1 H, d, *J* = 2 Hz); mass spectrum *M*⁺ 383 (45.1%), *M*⁺ - CH(CN)₂ 318 (57.5%), *M*⁺ - (TCNE H) 254 (100%).

Photolysis of 2 in Diethylamine. A solution of 100 mg (0.35 mmol) of 2 in 130 mL of diethylamine was irradiated for 30 min under nitrogen atmosphere. The crude products were separated on a Lobar column with *n*-hexane-dichloromethane (4:1, v/v) elution. Two peaks were obtained at elution times of 6 and 8 min. The first fraction gave 27.5 mg (25% yield) of 2-(dimethylamino)-3-(9-fluorenyl)pyridine (15): colorless prisms; mp 155–155.5 °C; ¹H NMR (CDCl₃) δ 1.22 (6 H, t, *J* = 7.5 Hz), 3.40 (4 H, q, *J* = 7.5 Hz), 5.80 (1 H, s), 6.72 (2 H, d, *J* = 4 Hz), 7.2–7.6 (6 H, m), 7.84 (2 H, d, *J* = 7 Hz), 8.28 (1 H, dd, *J* = 4, 3 Hz); mass spectrum *M*⁺ 314 (100%), *m/e* 285 (53%); calcd for C₂₂H₂₂N₂ 314.1781, found 314.1770.

The second fraction was 2-(diethylamino)-3-(9-fluorenylidene)-3H-azepine (14): 11 mg (10% yield); yellow oil; ¹H NMR (CDCl₃) δ 0.92 (3 H, t, *J* = 7.2 Hz), 1.34 (3 H, t, *J* = 7.2 Hz), 3.12 (1 H, q, *J* = 7.2 Hz), 3.60 (3 H, m), 5.68 (1 H, t, *J* = 7 Hz), 6.34 (1 H, d, *J* = 10 Hz), 6.64 (1 H, dd, *J* = 10, 6 Hz), 7.16 (1 H, d, *J* = 7.5 Hz), 7.2–7.4 (4 H, m), 7.6–7.8 (2 H, m), 7.8–8.0 (1 H, m), 8.0–8.2 (1 H, m);



mass spectrum *M*⁺ 326.0 (100%), *m/e* 161.0 (31.7%); calcd for C₂₃-H₂₂N₂ 326.1784, found 326.1806.

ESR Measurements at Cryogenic Temperatures. ESR spectra were recorded on a Varian E-112 EPR spectrometer (9.30 GHz) equipped with an optical cavity accessory and an Oxford cryostat, the latter being connected with a helium reservoir through a transfer tube. The signal positions were recorded with the aid of a Gaussmeter (Varian E-500). The sample solutions were degassed by freeze-thaw cycles in a quartz tube of 4-mm diameter. Irradiation was carried out by a high-pressure mercury lamp (Ushio USH-500 D) through a cylindrical quartz cell (50 mm in diameter and 50 mm in depth) filled with distilled water to absorb radiative heat. A light beam was focussed on a sample tube in the cavity through a quartz lens (*f* = 10 cm).

Quantum Yield Measurements of the Photorearrangement. Quantum yields of the photorearrangements of 1 were determined with the monochromatic light of 5-nm dispersion obtained by using an Ushio UXL-500D 500W xenon lamp and a Shimadzu 33-86-25 monochromator. The energy of the absorbed light was determined by a power meter (International Light, Inc., IL 700A) in an integral mode as the difference

of the transmitted light energy between the solution and the solvent. The power meter was calibrated by the photolysis of phenyl azide in hexane at 25 °C for which Φ = 0.53 at 254 nm. The photochemical conversion of 1 was determined by HPLC.

Time-Resolved Spectral Measurements on Triptycene. A degassed solution of triptycene in cyclohexane (5.3 × 10⁻⁴ M) was irradiated in a 1 × 1 × 4 cm quartz cell with a 248-nm pulse from a KrF excimer laser (Lamda Physik EMG 500) with a pulse width of 10 ns (fwhm) and output energy of 60 mJ/cm². The monitoring light source for the transient absorption spectra was an EG & GFCX-265 UV-xenon lamp.¹⁴ The monitoring light was divided into two beams, one of which was used for normalization of the transient absorption. The sample was renewed at each shot.

Fluorescence and Excitation Spectra Measurements of Triptycenes. A 2,2-dimethylbutane-pentane (8:3 v/v) solution of triptycene or 1-aza-triptycene (ca. 1 × 10⁻⁵ mol/L) was placed in a quartz cell of 1.0-cm optical length. Dissolved oxygen was removed by 3 freeze-thaw cycles. Fluorescence and excitation spectra were recorded on a Shimadzu RF-502 spectrometer at 25 °C. The same sample was immersed in a liquid nitrogen Dewar vessel with transparent windows. The vessel was placed in a sample chamber of the spectrometer, and fluorescence and excitation spectra were recorded at 77 K.

Theoretical Calculations. The Pariser-Parr-Pople method within the zero-differential-overlap approximation was used for the calculation of the π-electron densities and bond orders of 6. The parameters used in these calculations were as follows: *I*_C = 11.16, *I*_N = 14.16, γ_{CC} = 11.34, γ_{NN} = 12.82, β_{CC} = -1.7901, and β_{CN} = -2.57 eV. The Hückel parameters for initial guess were *h* = 2.0 and *k* = 1.0 in α_N = α_C + *h*β_{CC} and β_{CN} = *k*β_{CC}. All the C-C and C-N bond lengths were assumed to be 1.39 and 1.36 Å, respectively. The bond angles of the cyclopent[*cd*]-azulene moiety were taken close to those of the crystal structure of related hydrocarbons. The bond angles of the annulated benzene rings were assumed to be 120°. Calculations were carried out on a Hitachi M-200H computer, using a "SCF-CI-PI-MO program with PPP approximation" programmed by Mueller-Westerhoff and filed in the program library of the computer center of IMS.

MINDO/3 calculations of the MO's of 1-azabarrelene were carried out on the basis of the following geometries: C-N = 1.46 Å, C-C = 1.50 Å, C-H = 1.10 Å, C=C = 1.34 Å, ∠NCC = ∠CCC = 114°, and ∠CCH being optimized. A Hitachi M-200H computer was used for the program "MO calculation by MINDO/3 method" filed by S. Kato and S. Nagase.

Acknowledgment. This work was supported partly by the Grant-in-Aid for Cooperative Research (A) (Project No. 00534020) from the Ministry of Education, Science and Culture of Japan. We are grateful to Prof. K. Yoshihara and Dr. N. Nakashima of IMS for their kind help in obtaining the S_n ← S₁ absorption spectra.

Registry No. 1, 197-45-5; 2, 74357-30-5; 3, 74357-27-0; 4, 74368-32-4; 5, 74368-33-5; 6, 94427-07-3; 7, 94427-09-5; 8, 94427-10-8; 9, 386-77-6; 10, 74357-31-6; 11, 94427-11-9; 12, 94427-12-0; 13, 94427-13-1; 14, 75819-53-3; 15, 74357-28-1; 16, 13395-89-6; 17, 16783-54-3; 18, 94427-08-4; DBH, 4670-86-4; TCNE, 670-54-2; trityl tetrafluoroborate, 341-02-6; diethylamine, 109-89-7; phenyl azide, 622-37-7; 2-methylphenyl azide, 31656-92-5; 2,4-dimethylphenyl azide, 35523-91-2; 2-*tert*-butylphenyl azide, 20442-98-2; *o*-azidobiphenyl, 7599-23-7; 4-aza-1,1,2,2-tetracyano-9-methylspiro[2.6]nona-4,6,8-triene, 94427-14-2; 4-aza-1,1,2,2-tetracyano-9-*tert*-butylspiro[2.6]nona-4,6,8-triene, 94427-15-3; 4-aza-1,1,2,2-tetracyano-7,9-dimethylspiro[2.6]nona-4,6,8-triene, 94427-16-4; 4-aza-1,1,2,2-tetracyano-9-*tert*-butylspiro[2.6]nona-4,6,8-triene, 94427-17-5; 4-aza-1,1,2,2-tetracyano-9-phenylspiro[2.6]nona-4,6,8-triene, 94286-26-7; triptycene, 477-75-8; 18, 94537-19-6; acetic acid, 64-19-7.